Size tuning of Au nanoparticles formed by electron beam irradiation of Au_{25} quantum clusters anchored within and outside of dipeptide nanotubes†

Perumal Ramasamy,‡[a] Samit Guha,‡[b] Edakkattuparambil Sidharth Shibu,[a] Theruvakkattil S. Sreeprasad,[a] Soumabha Bag,[a] Arindam Banerjee*[b] and Thalappil Pradeep*[a]

Received 7th July 2009, Accepted 11th September 2009
First published as an Advance Article on the web 2nd October 2009
DOI: 10.1039/b913405k

Glutathione protected Au_{25} quantum clusters, exhibiting characteristic fluorescence, have been uniformly coated inside and outside of β-Ala-L-Ile dipeptide nanotubes. These coated structures have been imaged using the inherent fluorescence of Au_{25}. Upon exposure to an electron beam, in a transmission electron microscope, the quantum clusters gradually transform to gold nanoparticles, of the metallic size regime. The nanoparticles grow to a size of 4.5 nm and thereafter the particle size is unaffected by electron beam exposure. The nanotubes are intact and this template is shown to control the uniformity of the size of the nanoparticles grown. The quantum clusters can be loaded selectively inside the tubes using capillarity of the nanotubes. The sizes of the nanoparticles grown are tuned using electron beam exposure.

Introduction

The discovery of carbon nanotubes (CNTs)[1] has prompted a great deal of research in the construction of hollow nanotubular structures, including inorganic[2] and organic nanotubes.[3] Peptide-based nanotubular structures belong to an important class of nanotubes due to their probable use in biological and medical sciences including glucose transporters, transmembrane pores, ion channels, potential antibiotics, separation/preservation/storage of drugs and others.[4] Design and construction of cyclic oligopeptide-based nanotubular structures have been pioneered by Ghadiri and coworkers.[5] In recent years, dipeptide nanotubes (DPNTs), interesting candidates in the plethora of soft nanobiotubular structures, have been introduced.[6] Such structures can acquire new properties by the incorporation of nanoparticles. However, formation of organic nanotube-inorganic nanoparticle based hybrid nanomaterials with desired functions remains a challenge in nanotechnology.[7–13]

Matsui and co-workers have reported self-assembling nanotube/metal nanoparticle (Au, Ag, Pt, Cu and Ni) hybrid materials.[9] They have also reported size controlled Au and Cu nanocrystal growth on nanotubes and this was done by tuning conformations and charge distribution of histidine-rich peptide templates.[9a,c] In their study, they demonstrated that the size of Ag nanocrystals was increased by increasing ion incubation time.[9b] Gazit and co-workers have reported Phe-Phe DPNTs and these nanotubes have been used as scaffolds for producing silver nanowires within the channels.[7a] These silver-filled DPNTs were further coated with gold nanoparticles on the surface of peptide nanotubes using linker peptides to achieve metal-insulator-metal trilayer coaxial nanocables. Shelnutt and co-workers have reported DPNT/platinum nanoparticle composites.[8] Recently some of us have also reported robust crystalline DPNTs and these nanotubes have been found to be suitable templates for fabricating dipeptide capped gold nanoparticles on the outer surface of these nanotubes.[10] These DPNTs are thermally stable, pH stable, enzymatically stable and are crystalline.[10]

Au quantum clusters with size below 2 nm are an emerging field of current research owing to their fascinating properties including photoluminescence,[14] optical chirality,[15] ferromagnetism,[16] quantized double layer charging behavior[17] as well as potential applications such as single molecule optoelectronics,[18] sensing,[19] and bioassays.[20] Au quantum clusters are extremely sensitive to the electron beam.[23] Herein we report electron beam induced formation of Au nanoparticles from Au_{25} quantum clusters within and outside of DPNTs. Hydrogen bonding functional groups of DPNTs play a crucial role in the formation and stabilization of nanoparticles. Several researchers have tried to incorporate metal particles inside the nanotubes. Early work on bismuth and lead relied upon capillary action to pull liquids into the hollow nanotube cavities.[21a,b] In the present work, by using an overnight diffusion technique through the capillary effect, the inside regions of the tubes are filled with Au clusters. They are also deposited uniformly on the outside surface of the tubes. Upon exposure to the electron beam in a transmission electron microscope, the quantum clusters become unstable, leading to the formation of nanoparticles of ~4 nm diameter; in other words, there exists a quantum cluster to metallic particle transformation. Thus, metal (Au cluster)-insulator (peptide

[a]*DST Unit on Nanoscience, Department of Chemistry and Sophisticated Analytical Instrument Facility, Indian Institute of Technology Madras, Chennai, 600 036, India. E-mail: pradeep@iitm.ac.in; Fax: +91-44 2257-0545*

[b]*Department of Biological Chemistry, Indian Association for the Cultivation of Science, Jadavpur, Kolkata, 700032, India. E-mail: bcab@iacs.res.in; Fax: (+)91-33-2473-2805*

† Electronic supplementary information (ESI) available: EDAX analysis of DPNTs with gold before exposure to electron beam, EDAX analysis of DPNTs with gold after exposure to electron beam, size distributions of gold nanoparticles in DPNT/Au composite with respect to 100 keV electron beam exposure time and schematic representation of the formation of uniform gold nanoparticles on DPNTs due to exposure to electron beam. See DOI: 10.1039/b913405k

‡ These two authors have contributed equally.

nanotube)-metal (Au cluster) trilayer[7b,9d,22] hybrid materials have been obtained as the nanoparticles are present on the inner and outer surfaces of the insulating nanotubes. A major advantage of this technique is that the size of the aggregated Au cluster on the nanotube template can be efficiently, uniformly and reproducibly controlled by tuning the electron beam exposure time. Besides, the transformation can be effected in specific regions of the nanotubes using spatial control of the electron beam.

Experimental

$Au_{25}SG_{18}$ was synthesized according to the reported method.[23] Gluthathione (GSH), γ-Glu-Cys-Gly, exists in the thiolate form on the cluster. This protection makes the compound water-soluble. As a result, the cluster can be incorporated onto DPNTs to make the latter fluorescent, as Au_{25} is inherently fluorescent.[23] DPNTs were synthesized as reported by Guha and Banerjee.[10] They were dispersed in water (3mg mL^{-1}). To this, varying concentrations of Au_{25} clusters were added. The solution containing the nanotube and gold clusters was incubated at room temperature for a day. Raman spectra were measured using a WiTec GmbH confocal micro Raman. The excitation wavelength used was 532 nm. For collecting Raman spectra, the samples were prepared by drying the solution containing the nanotubes and Au_{25} clusters on a cover glass. The nanoscale features of the DPNTs were studied using AFM. For AFM measurements, the samples were prepared using an aqueous solution (3 mg mL^{-1}) on a mica sheet by slow evaporation and vacuum drying at room temperature for 2 days. AFM images were recorded using an AUTOPROBE CP BASE UNIT DI CP-II instrument (model no: AP-0100). Fluorescence measurements were made using an Olympus, 1 × 2-KSP, 6M 24413, Japan. The samples were prepared by drying an aqueous solution (3 mg mL^{-1}) on a cover glass. The wavelength used for excitation was 530–550 nm. The samples for TEM were prepared by dropping the dispersion on amorphous carbon films supported on a copper grid and drying in air for 2 days. These samples were examined using a JEOL 3011, 300 kV transmission electron microscope equipped with a UHR pole piece. In order to slow the beam induced damage, several measurements were carried out at a reduced energy of 100 keV. This was done also to observe the beam-induced effects more carefully.

Results and discussion

Au_{25} gold clusters

Au_{25} gold clusters have a core diameter of 0.7 nm and are very sensitive to the electron beam.[23] The clusters exhibit inherent fluorescence and solid-state emission.[23] The solid state emission from the clusters is found to be temperature dependent.[23] The optical absorption spectrum has a maximum at 672 nm. This is due to the LUMO ← HOMO transition derived from the intraband (sp) states, while the features at lower wavelengths are due to interband transitions (sp ← d). Photoluminescence measurements show that the Au_{25} clusters have an excitation maximum at 535 nm and emission maximum at 700 nm. The quantum yield of the cluster is 1.9×10^{-3}.[23b]

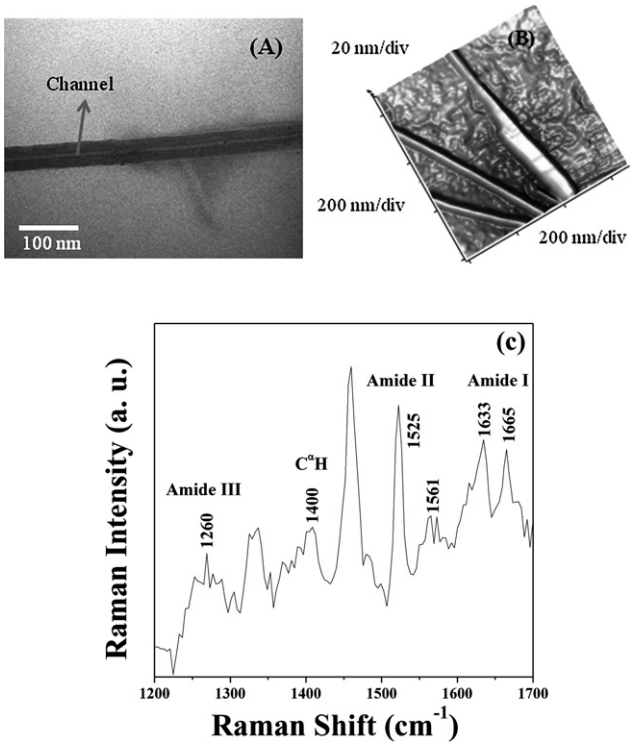

Fig. 1 (A) TEM image, (B) AFM image and (C) Raman spectrum of hollow nanotubular structures formed by the dipeptide, β-Ala-L-Ile.

Dipeptide nanotubes

TEM experiments were performed to investigate the morphological features of the dipeptide. The TEM image shown in Fig. 1A shows a hollow nanotube with 36 nm total diameter with a 6 nm inner channel. Inside the nanotube appeared lighter indicating that it is hollow. The features of the nanotube are the same as those already reported by some of us earlier.[10]

AFM measurements

We have also studied noncontact-mode AFM (Fig. 1B) to investigate the morphological features and 3D structure of the nanotube. The image gives a 3D view of the nanotubes formed from self-association of the dipeptide, β-Ala-L-Ile. Of the three tubes in Fig. 1B, two are uniform while the third is not so due to two tubes meshed together for half the length.

Raman spectra and Raman images of nanotubes

The Raman spectra for the DPNTs in aqueous solution show peaks at 1665 and 1633 cm^{-1} due to amide I, 1561 and 1525 cm^{-1} due to amide II, 1400 cm^{-1} due to $C^{\alpha}H$ and 1260 cm^{-1} due to amide III bands, indicating a β-sheet structure (Fig. 1C).[24] This β-sheet structure can be folded along one axis of the two-dimensional layer using intermolecular hydrogen bonding to form nanotubular structures in solution.[10] Long needle-like (tens of μm in length) morphology was observed when the samples were dried on a cover slip and the dipeptide showed a broad luminescence peak centered at 1930 cm^{-1} (595 nm) in the Raman spectrum (Fig. 2A). The appearance of this broad peak could be

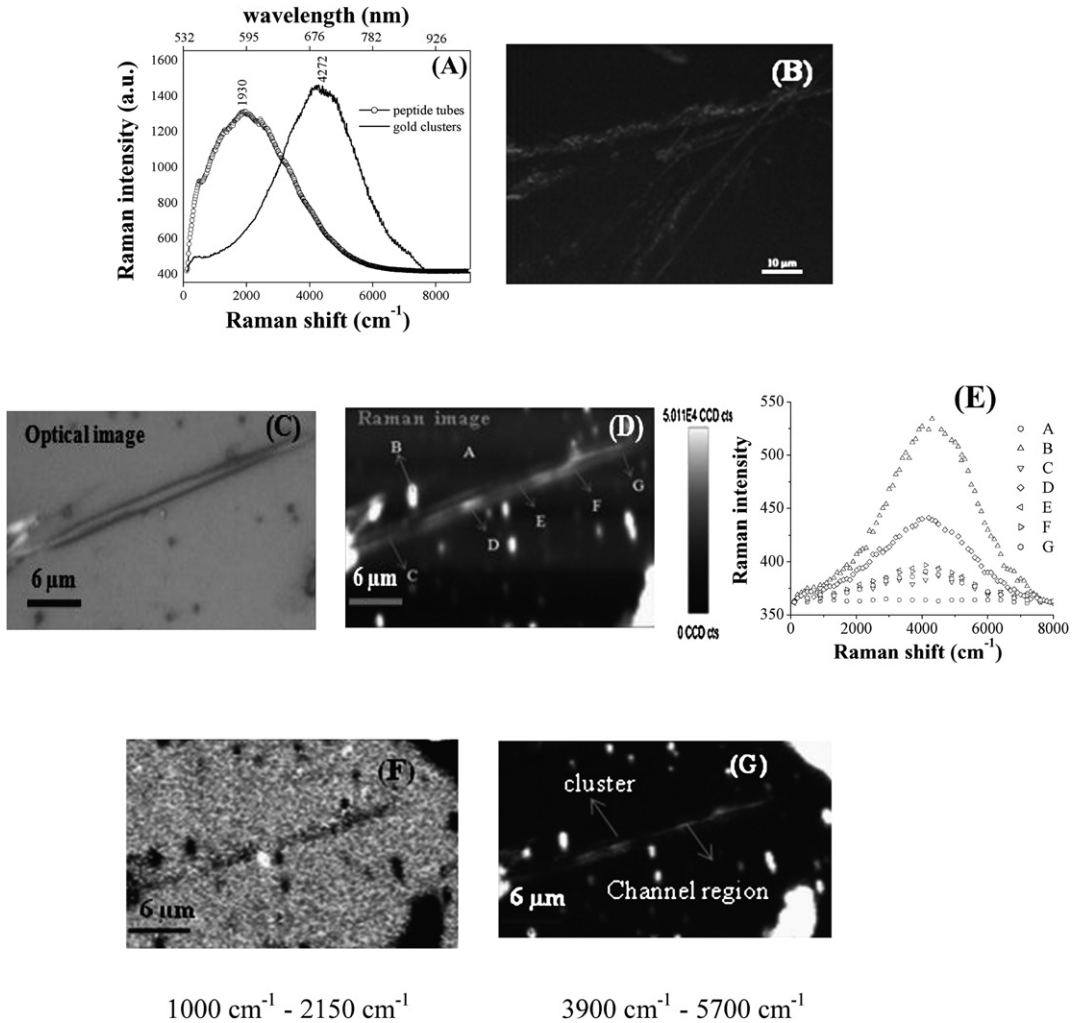

Fig. 2 (A) Fluorescence Raman spectra of DPNTs and Au clusters, (B) fluorescence image of DPNTs/Au composite, (C) optical image of DPNTs/Au composite, (D) Raman image of DPNTs/Au composite, (E) Raman spectra at different regions in (D), (F) extracted peptide rich region from (D), (G) extracted cluster rich region from (D).

due to self-assembly of these dipeptide tubes. In contrast, the Raman spectrum for Au_{25} clusters has a broad peak centered at 4272 cm^{-1} due to fluorescence at 690 nm (Fig. 2A). This value matches with the solid state emission of Au_{25}.[23a]

Fluorescence measurements

Fig. 2B shows the fluorescence image of the DPNTs/Au quantum clusters (excited at 530–550 nm) where several self-assembled fluorescent tubes are clearly visible. The tubular nanocomposites clearly exhibited fluorescence originating from the electronic transition of the Au quantum clusters. The relative homogeneity of the fluorescence signal in a one-dimensional fashion also implies that the Au quantum clusters are uniformly coated on the DPNTs.

Raman spectra and Raman images for dipeptide tubes with gold clusters

Fig. 2C and D show optical and Raman images of a region in the sample containing peptide tubes with gold clusters with a 1:0.2 weight ratio. These were collected using a Witec Raman microscope. Fig. 2E shows the spectra at different regions of the sample.

It is observed that only the fluorescence signal for gold is observed at different regions along the tube. Since the fluorescence intensity is nearly the same at regions like C, E, F and G marked in Fig. 2D, we feel that the tube is uniformly coated in most of the regions of the tube. Also it is observed that at some places in the tube (D), there is more fluorescence. This suggests that some gold clusters could be trapped inside the tube.

For greater clarity on the distribution of gold on/in the tube, we used the following method. As the broad fluorescence for dipeptide nanotubes is centered around 1930 cm^{-1} and the fluorescence peak position for gold clusters is centered around 4272 cm^{-1} (for 532 nm excitation), in order to distinguish the regions that are rich in dipeptide tubes from those having clusters, the Raman intensities in the 1000 cm^{-1}–2150 cm^{-1} and 3900 cm^{-1}–5700 cm^{-1} region were mapped. These are expected to show the dipeptide (Fig. 2F) and nanocluster (Fig. 2G) regions. From Fig. 2F, it is clear that almost no Raman signal for

dipeptide is observed and the image is dark while the Au cluster is observed all over the tube (Fig. 2G). The intensity due to the Au clusters is almost the same on the periphery of the tube. This shows that the Au clusters are uniformly coated on the surface of the tube. It can also be seen that the channel region of the tube has higher intensity and therefore indicates that Au clusters are present inside the tube throughout the channel. It can also be observed that their intensity is same throughout the length of the channel indicating uniformity of the gold cluster distribution due to the capillary effect.

Electron beam induced formation of nanoparticles on peptide tubes

Au clusters are extremely sensitive to the electron beam which causes aggregation to yield larger nanoparticles upon longer exposure. A series of TEM images were analyzed to understand the electron beam assisted growth of glutathione capped Au quantum clusters on dipeptide nanotube templates. Solutions containing peptide nanotubes and Au clusters were combined in the ratio 1:1. The material was then incubated at room temperature overnight. The solution was placed as a droplet on a carbon coated copper grid (300 mesh) and then slowly vacuum dried at 30 °C for 2 days. It was then exposed to the electron beam in the TEM for different periods (Fig. 3A). In order to reduce beam induced damage to the nanotubes, the electron beam exposure was carried out at 100 keV. It was observed that size of the Au clusters increased with exposure time. Unexposed Au clusters on the DPNT template did not increase in size. Since the concentration of gold clusters is high, only the particles formed on the surface of the peptide tube were observed. Prolonged exposure (for 45 min) showed discrete nanoparticles and the peptide tube was not clearly observable. If exposure to electron beam decomposes DPNT, then the elements C, N and O will be absent after electron beam exposure. However, EDAX data show that C, N and O are present both before and after (45 min) exposure to the electron beam (ESI,† Fig. S1 and S2), although the presence of C is partly due to the grid. We have also tried Raman spectroscopy and Raman imaging and it was clear that the nanotubes are stable upon exposure to the beam for a long time. However, as it is almost impossible to get the same dipeptide tube for Raman investigation after electron beam exposure, these results have some uncertainty. The invisibility of the edges of DPNT in the presence of gold is due to the greater contrast of gold and not due to degradation of the nanotube. This structural and chemical stability of the DPNTs with the incorporation of clusters in the presence of the electron beam is important as it leads to the fabrication of metal-insulator-metal trilayer coaxial nanocables. However, the similarity of the materials distributions of the elements before and after exposure suggests that the nanotubes are stable.

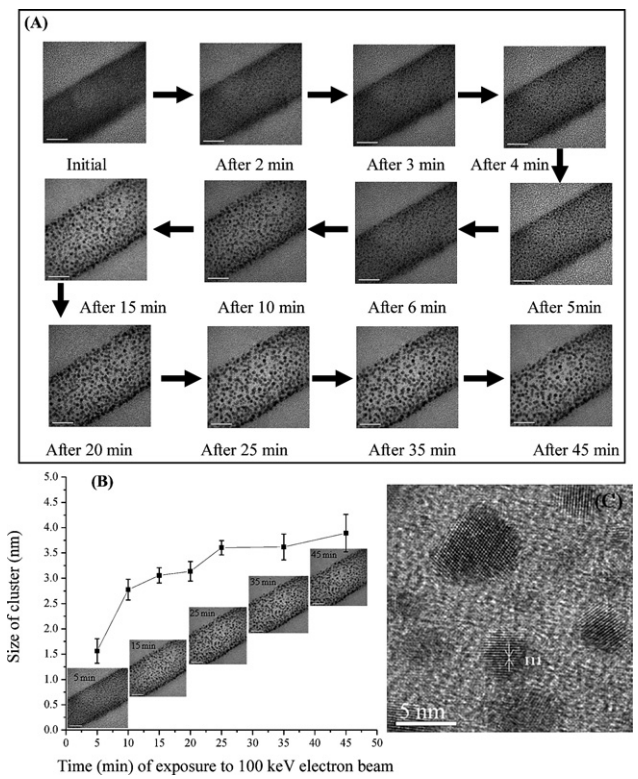

Fig. 3 (A) Formation of gold nanoparticles due to the exposure of the gold clusters anchored on a dipeptide tube to the electron beam and (B) size distribution of particles in (A). The scale bars in (A) and (B) correspond to 20 nm. (C) TEM image of the gold nanoparticles after electron beam exposure for 45 minutes.

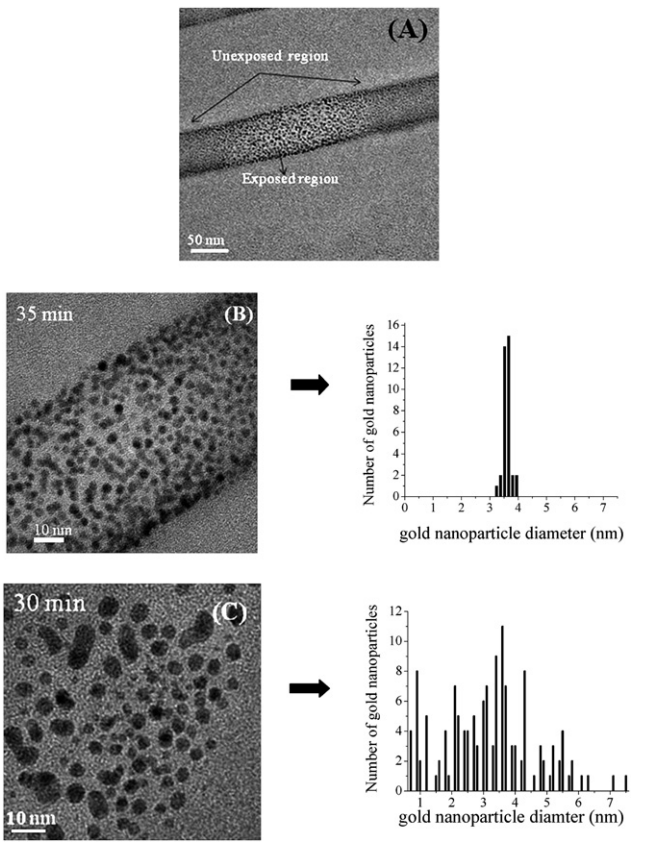

Fig. 4 (A) TEM image of DPNTs/Au nanocomposite showing regions that were both exposed and unexposed to the 100 keV electron beam for 45 min. (B,C) Comparison of size distributions of nanoparticles upon their growth from clusters for (B) with (35 min) and (C) without (30 min) DPNTs. 100 keV electron beam was used.

Evolution of size of Au particles on DPNTs

Fig. 3B is a plot of the variation in size of the nanoparticles as a function of exposure time. It is observed that most of the particles are spherical and the particle size increases till about 45 minutes and reaches a maximum of ~4 nm at the end of 45 minutes. At this size, the particles are metallic. For any given exposure time, it is observed that the particles are uniform in size (ESI,† Fig. S3). A TEM image of the particles (Fig. 3C) shows the lattice planes clearly. The d spacing observed for almost all the nanoparticles is 2.35 Å, due to the (111) plane of Au. The lattice planes are oriented in different directions for the particles. Due to the high energy of the electron beam, it functions as an efficient, focused heating source for the Au_{25} clusters and leads to the coalescence, nucleation and growth of the Au clusters within and outside of the nanotubes. The reason why on the dipeptide tube surface the Au nanoparticles have a uniform diameter of ~4 nm while Au nanoparticles formed without nanotubes have a wider size distribution is because of the limited amount of Au_{25} clusters on the tube surface which is determined by surface functional groups, surface area and surface curvature. Aggregation and migration alone may not lead to the formation of single-crystalline Au nanoparticles. It is observed that the interparticle separation is ~4.5 nm on the dipeptide nanotube surface for all exposure times less than 90 minutes. This indicates the uniform distribution of gold clusters along the surface of the tube which coalesce, nucleate and grow to form nanoparticles. The exposed and unexposed regions of the tube containing the channel are shown in Fig. 4A. Clearly only the exposed regions show the growth of nanoparticles. It is also clear that the nanotube does not show any disturbance due to exposure. We have measured the aggregated Au cluster size after electron beam exposure with and without DPNTs (Fig. 4B, C). It is interesting to note that for clusters with DPNTs (35 min electron beam exposure time) the particle size distribution is homogeneous (3–4 nm), while for clusters without DPNTs (30 min electron beam exposure time) it is highly heterogeneous (0.7–7.5 nm). Therefore, the nanotube template has a significant influence on regulating the size of Au clusters. Most probably, these GSH capped Au clusters are further stabilized by the functional groups (NH_2 and COOH) present in DPNTs.[10]

Possible explanation for the formation of uniform nanoparticles on DPNTs

When DPNTs are mixed with GSH capped Au clusters in solution, the Au clusters are further stabilized by the functional groups (NH_2 and COOH) present in the DPNTs. The functional groups are distributed uniformly throughout the tube. Hence a uniform layer of GSH capped Au clusters is formed on the DPNTs. Upon exposure to the electron beam, the inherent instability of the quantum clusters when exposed to the electron beam favors coalescence, nucleation and growth of Au nanoparticles of uniform sizes with an interparticle separation of ~4.5 nm. Hence the chemistry of the surface of the DPNT, available surface area and surface curvature plays a crucial role in providing stability for the formation of a uniform layer of GSH capped Au clusters upon it, while the inherent instability of the quantum clusters to the electron beam favors the formation of nanoparticles. This implies that the nanoparticle size can be tuned using the electron beam. This is schematically illustrated in ESI† 4.

Capillarity effect

We sonicated the DPNTs/Au cluster composite. However, after sonication, a one-dimensional array was not observed because sonication may disrupt nanotube formation. In order to incorporate the gold clusters inside the channels, we reduced the concentration of gold clusters and utilized the capillarity effect on gold clusters added to the DPNTs. An aqueous solution containing the peptide tubes was mixed with gold clusters in a 1:0.2 weight ratio. The mixture was incubated at room temperature overnight. If the core of the nanotube is completely

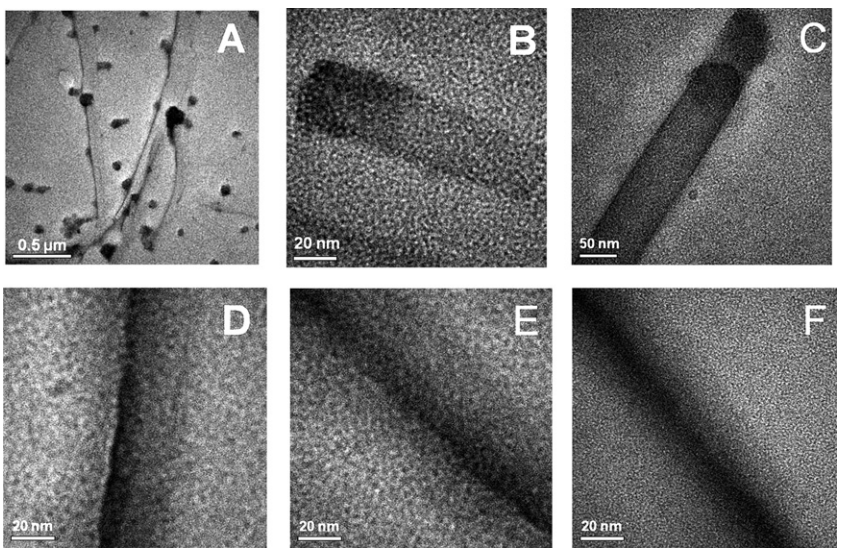

Fig. 5 (A) DPNT/Au composite, (B) and (C) DPNTs with clusters at the openings of the tubes, (D)–(F) DPNTs having gold clusters inside their channels indicating the capillarity effect.

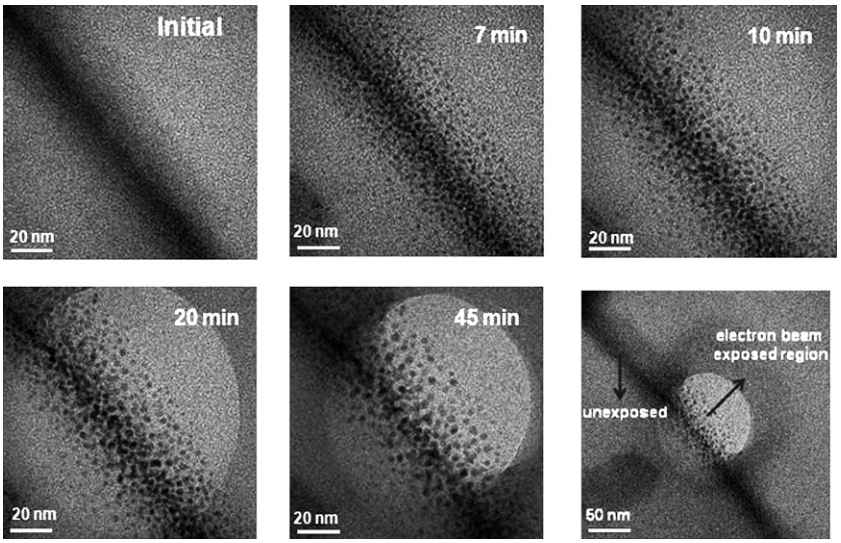

Fig. 6 Evolution of the Au nanoparticles within a nanotube channel from electron beam exposure (100 keV).

hollow, the contrast inside the nanotube should appear as a lighter color as shown in the TEM image (Fig. 1A) of the DPNT. More than one tube/Au cluster composite was observed and some of the cluster bundles were attached to the surface of the tubes (Fig. 5). In some tubes, the end of the tube was closed due to the Au clusters (Fig. 5B, C). In several tubes, it was observed that the inner channel was filled with Au clusters (Fig. 5D–F). These indicate the capillarity effect. Upon exposure to 100 keV electron beam, nanoparticles grew inside the DPNTs. The average interparticle spacing was ~4.5 nm near the outer edge of the tube. However, the channel region has particles that are almost continuously distributed. For tubes with their channels filled with gold clusters, the outer tube surface could not be clearly observed when compared to the inner channel. A darker contrast was observed due to the aggregated Au quantum cluster growth inside the nanotube template. This indicates that the electron beam is intense enough to aggregate the particles even inside the tube. The concentration of clusters inside the tube is more than the outside surface and it indicates that the gold clusters entered the inside of these tubes due to the capillarity effect. The exposed and unexposed regions of the tube containing the channel are also shown in Fig. 6. The electron beam exposed part of the tube alone grows into metallic nanoparticles. However, the transformed region could not be analyzed using other probing techniques as this transformation is induced only in a few tubes on the TEM grid, on length scales in the range of tens of nanometers, rendering it very hard for detection using other analyzing techniques. This is especially the case as other studies are ex-situ, done post-TEM examination.

Conclusion

Uniform deposition of glutathione (GSH) protected Au_{25} quantum clusters inside and outside of DPNTs has been achieved and the size of the coalesced Au clusters has been tuned using electron beam irradiation. This has been achieved by taking advantage of the chemical stability of DPNTs for functionalization of glutathione capped Au quantum clusters and by size-tuning the Au clusters which are unstable to high energy electron beams. Unexposed Au clusters do not change with time indicating that this method may be utilized not only to create organic/inorganic hybrid nanocomposite systems but also to regulate the size of the aggregated metal clusters on the nanotube surface. Moreover, on the same nanotube, different regions of the tube can have different sizes of aggregated Au clusters depending on the electron beam exposure time. A capillary effect triggers the entry of Au clusters inside the peptide nanotubes and it helps to create metal (Au nanoparticle inside the channel)-insulator (peptide nanotube)-metal (Au nanoparticle on the surface) trilayer[7b,9d,22] hybrid materials successfully, using an overnight diffusion technique and subsequent electron beam irradiation, suggesting a probable use of this composite in making nanodevices. The uniqueness of this technique is in the size control of aggregated Au clusters on DPNT templates and modulation of this size to different extents in different regions of the same nanotube template by electron beam irradiation.

Acknowledgements

We thank the Nanoscience and Nanotechnology Initiative of DST, Government of India, for supporting our research program.

References

1 S. Iijima, *Nature*, 1991, **354**, 56–58.
2 R. Tenne, L. Margulis, M. Genut and G. Hodes, *Nature*, 1992, **360**, 444–446.
3 T. Shimizu, M. Masuda and H. Minamikawa, *Chem. Rev.*, 2005, **105**, 1401–1443.
4 (*a*) J. R. Granja and M. R. Ghadiri, *J. Am. Chem. Soc.*, 1994, **116**, 10785–10786; (*b*) D. Ranganathan, *Acc. Chem. Res.*, 2001, **34**, 919–930.
5 T. D. Clark, J. M. Buriak, K. Kobayashi, M. P. Isler, D. E. McRee and M. R. Ghadiri, *J. Am. Chem. Soc.*, 1998, **120**, 8949–8962.
6 M. Yemini, M. Reches, J. Rishpon and E. Gazit, *Nano Lett.*, 2005, **5**, 183–186.
7 (*a*) M. Reches and E. Gazit, *Science*, 2003, **300**, 625–627; (*b*) O. Carny, D. E. Shalev and E. Gazit, *Nano Lett.*, 2006, **6**, 1594–1597.

8 Y. Song, S. R. Challa, C. J. Medforth, Y. Qiu, R. K. Watt, D. Peña, J. E. Miller, F. van Swol and J. A. Shelnutt, *Chem. Commun.*, 2004, 1044–1045.
9 (*a*) R. Djalali, Y. Chen and H. Matsui, *J. Am. Chem. Soc.*, 2003, **125**, 5873–5879; (*b*) L. Yu, I. A. Banerjee and H. Matsui, *J. Am. Chem. Soc.*, 2003, **125**, 14837–14840; (*c*) L. Yu, I. A. Banerjee, M. Shima, K. Rajan and H. Matsui, *Adv. Mater.*, 2004, **16**, 709–712; (*d*) I. A. Banerjee, Lingtao Yu and H. Matsui, *Proc. Natl. Acad. Sci. U. S. A.*, 2003, **100**, 14678–14682.
10 S. Guha and A. Banerjee, *Adv. Funct. Mater.*, 2009, **19**, 1949–1961.
11 B. C. Satishkumar, A. Govindaraj, M. Nath and C. N. R. Rao, *J. Mater. Chem.*, 2000, **10**, 2115–2119.
12 (*a*) S. S. Bale, P. Asuri, S. S. Karajanagi, J. S. Dordick and R. S. Kane, *Adv. Mater.*, 2007, **19**, 3167–3170; (*b*) B. H. Juárez, C. Klinke, A. Kornowski and H. Weller, *Nano Lett.*, 2007, **7**, 3564–3568.
13 A. Wu, W. Cheng, Z. Li, J. Jiang and E. Wang, *Talanta*, 2006, **68**, 693–699.
14 T. P. Bigioni, R. L. Whetten and O. Dag, *J. Phys. Chem. B*, 2000, **104**, 6983–6986.
15 I. L. Garzon, J. A. Reyes-Nava, J. I. Rodriguez-Hernandez, I. Sigal, M. R. Beltran and K. Michaelian, *Phys. Rev. B: Condens. Matter Mater. Phys.*, 2002, **66**, 073403.
16 P. Crespo, R. Litran, T. C. Rojas, M. Multigner, J. M. de la Fuente, J. C. Sanchez- Lopez, M. A. Garcia, A. Hernando, S. Penades and A. Fernandez, *Phys. Rev. Lett.*, 2004, **93**, 087204.
17 S. Chen, R. S. Ingram, M. J. Hostetler, J. J. Pietron, R. W. Murray, T. G. Schaaff, J. T. Khoury, M. M. Alvarez and R. L. Whetten, *Science*, 1998, **280**, 2098–2101.
18 T. H. Lee, J. I. Gonzalez, J. Zheng and R. M. Dickson, *Acc. Chem. Res.*, 2005, **38**, 534–541.
19 C. C. Huang, Z. Yang, K. H. Lee and H. T. Chang, *Angew. Chem., Int. Ed.*, 2007, **46**, 6824–6828.
20 R. C. Triulzi, M. Micic, S. Giordani, M. Serry, W. A. Chiou and R. M. Leblanc, *Chem. Commun.*, 2006, 5068–5070.
21 (*a*) P. M. Ajayan and S. Iijima, *Nature*, 1993, **361**, 333; (*b*) R. Seshadri, A. Govindaraj, H. N Aiyer, R. Sen, G. N. Subbanna, A. R. Raju and C. N. R. Rao, *Curr. Sci.*, 1994, **66**, 839.
22 N. Tesla, U. S. Patent 514167, 1894.
23 (*a*) E. S. Shibu, M. A. H. Muhammed, T. Tsukuda and T. Pradeep, *J. Phys. Chem. C*, 2008, **112**, 12168–12176; (*b*) M. A. H. Muhammed, A. K. Shaw, S. K. Pal and T. Pradeep, *J. Phys. Chem. C*, 2008, **112**, 14324–14330.
24 V. Sikirzhytski, N. I. Topilina, S. Higashiya, J. T. Welch and I. K. Lednev, *J. Am. Chem. Soc.*, 2008, **130**, 5852–5853.

